International Journal of Nanomedicine

Dovepress
Taylor & Francis Group

Open Access Full Text Article

ORIGINAL RESEARCH

Royal Jelly Extracellular Vesicles Enhance Diabetic Wound Healing via Inflammation Modulation, Fibroblast Migration, and Angiogenesis

Yen-Yu Tsai[1], Long-Sen Chang[1], Chun-Wen Lan[1–3], Ying-Jung Chen[4–6], Jen-Hao Yang[1]

[1]Institute of Biomedical Sciences, National Sun Yat-Sen University, Kaohsiung, Taiwan; [2]SCT-Biomed Co., Ltd, Kaohsiung, Taiwan; [3]Department of Medical Education and Research, Kaohsiung Veterans General Hospital, Kaohsiung, Taiwan; [4]Department of Fragrance and Cosmetic Science, Kaohsiung Medical University, Kaohsiung, Taiwan; [5]Drug Development and Value Creation Research Center, Kaohsiung Medical University, Kaohsiung, Taiwan; [6]Department of Medical Research, Kaohsiung Medical University Hospital, Kaohsiung, Taiwan

Correspondence: Ying-Jung Chen, Kaohsiung Medical University, Kaohsiung, Taiwan, Tel +886 07 3121101 ext.2804, Email yjchen@kmu.edu.tw; Jen-Hao Yang, National Sun Yat-Sen University, Kaohsiung, Taiwan, Tel +886 07 5252000 ext.7104, Email jhyang1@mail.nsysu.edu.tw

Introduction: Diabetic wounds present a significant clinical challenge because of impaired healing and persistent inflammation. This study explored the therapeutic potential of extracellular vesicles derived from *Apis mellifera* royal jelly (RJEVs) to enhance diabetic wound repair.

Methods and Results: RJEVs were characterized using nanoparticle tracking analysis, transmission electron microscopy, and Western blotting. The results showed that RJEVs had a nanoscale size of approximately 118 nm and were characterized by a double-layered lipid membrane and extracellular vesicle markers CD63 and syntenin. In vitro, RJEVs significantly improved migration by 31.4 ± 4.4% and reduced senescence by 24.7 ± 5.8% in high-glucose-stimulated human dermal fibroblasts. Furthermore, RJEVs restored collagen type I protein expression by 41.9 ± 7.6% under hyperglycemic conditions. RJEVs also mitigated inflammation in lipopolysaccharide-stimulated macrophages and THP-1 cells by downregulating pro-inflammatory cytokines IL-1β, IL-6, IL-8, and TNF-α. Additionally, RJEVs restored endothelial cell migration by 35.7 ± 5.6% and tube formation by 36.1 ± 2.4% under hyperglycemic conditions, accompanied by increased expression of VEGF and CD31. In vivo, RJEVs treatment significantly accelerated wound closure in streptozotocin-induced diabetic porcine models by 32.5 ± 7.2% compared to the control group.

Conclusion: These findings indicate that RJEVs facilitate diabetic wound healing through the coordinated regulation of fibroblast function, immune modulation, and angiogenesis. This study introduces a nature-derived, non-mammalian extracellular vesicle platform with translational potential for chronic wound management in diabetes, offering a biocompatible and multifaceted therapeutic alternative to conventional approaches.

Plain Language Summary: Wound healing in patients with diabetes is often slow due to damaged blood vessels, excessive inflammation, and impaired fibroblast migration. Extracellular vesicles (EVs) are nanosized, membrane-bound bubbles that are released by cells. They carry materials such as proteins, DNA, and RNA to other cells to communicate and exchange information that impacts everything from tissue repair to disease development. In this study, EVs isolated from the superfood royal jelly (RJEVs), which is widely known for its antioxidant and anti-inflammatory effects, can accelerate diabetic wound healing in diabetic pigs. Further results from this study showed that RJEVs stimulated the formation of new blood cells and fibroblast migration and decreased inflammation in cellular conditions.

Keywords: skin, diabetes, high glucose, lipopolysaccharide, streptozotocin, porcine model

Introduction

Chronic wounds, particularly in patients with diabetes, represent a significant health and economic burden worldwide, affecting approximately 6.5 million patients annually,[1] with a prevalence rising among the elderly and diabetic

Received: 19 May 2025
Accepted: 10 October 2025
Published: 22 October 2025

Graphical Abstract

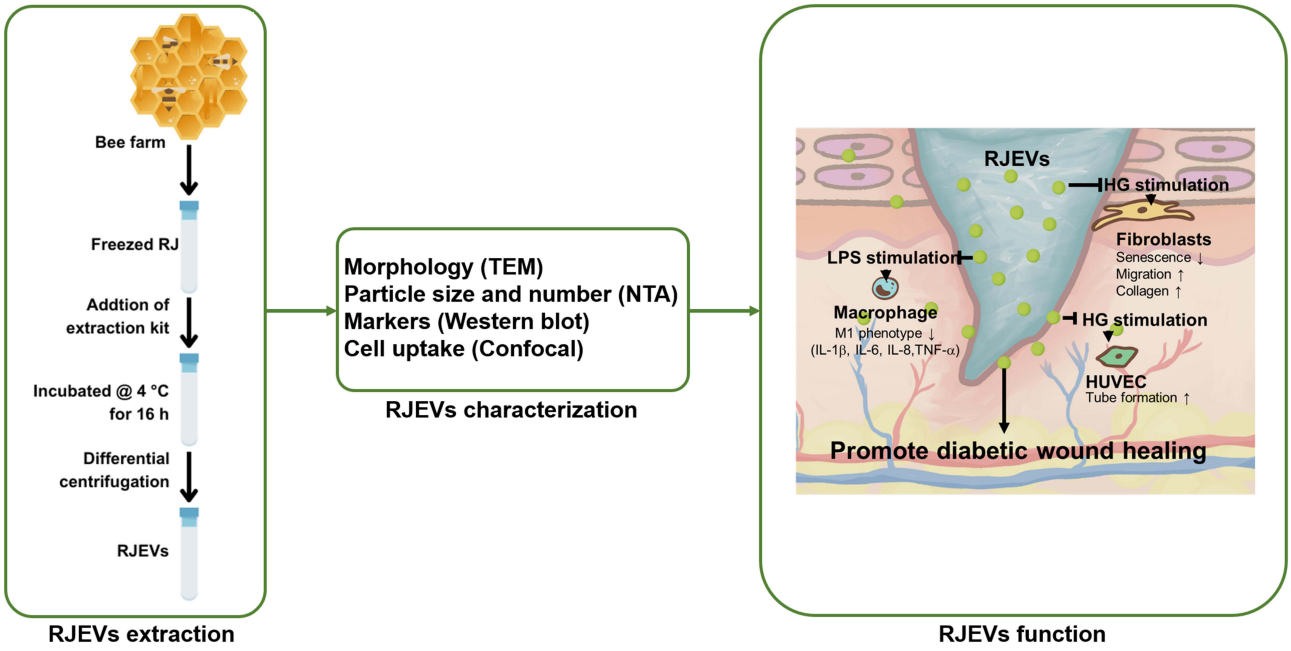

populations.[2,3] These wounds exhibit delayed healing and heightened infection risk, often resulting in severe complications such as amputation, which affects approximately 25% of individuals with diabetes.[4,5] Unlike the orderly progression of normal wound healing through inflammation, proliferation, and remodeling, diabetic wounds display persistent inflammation, reduced angiogenesis, impaired extracellular matrix formation, and delayed re-epithelialization.[6–8] These disruptions necessitate more intensive and targeted therapies,[9–11] as conventional approaches often prove insufficient.

Several in vivo studies have reported the potential therapeutic benefits of *Apis mellifera* royal jelly (RJ) in promoting diabetic wound healing by reducing inflammation and stimulating cell proliferation.[12–15] RJ is rich in proteins, lipids, vitamins, minerals, and bioactive compounds,[16] and major royal jelly proteins (MRJPs) constitute a significant portion of RJ as key components owing to their biological properties.[17] RJ is a source of essential amino acids and can prepare bioactive peptides with various functions, including antibacterial, antihypertensive, antioxidative, and anti-aging activities.[18] Although these preclinical findings are promising, clinical studies assessing the effects of RJ on diabetic wound healing remain limited and have demonstrated variable outcomes.[19–22] In this study, we focused on isolating extracellular vesicles (EVs) from RJ as a more biocompatible and scalable alternative to using whole RJ, which could be incorporated into advanced delivery platforms, such as hydrogels.

EVs are nanoparticles secreted by cells that deliver bioactive molecules to target cells.[23] Notably, studies have demonstrated the capacity of EVs to facilitate communication between species and kingdoms.[24] Royal jelly-derived EVs (RJEVs) have demonstrated remarkable wound-healing capabilities by influencing the differentiation and secretome of mesenchymal stem cells, thereby expediting wound healing in a splinted mouse model.[25] Additionally, RJEVs have demonstrated antibacterial effects, particularly against *Staphylococcus aureus* biofilm.[25,26] Interestingly, RJEVs regulate the expression of genes associated with cellular motility, viability, and apoptosis.[27]

This study is the first to investigate the potential of RJEVs as a novel therapeutic approach for diabetic wound healing, providing insights into the mechanisms of action and efficacy in addressing the complex interplay of factors that contribute to delayed healing in patients with diabetes mellitus (Supplementary Figure 1). The findings of this study are expected to pave the way for the development of more effective, targeted treatments for diabetic wounds, potentially

reducing healing time, lowering the risk of complications, and improving the quality of life of millions of diabetic patients using natural, biocompatible interventions that harness the body's innate healing process.

Materials and Methods

Reagents

The 4′,6-diamidino-2-phenylindole (DAPI blue) dye was acquired from Thermo Fisher Scientific (Waltham, Massachusetts, USA). Zeocin®, Normocin™, FSL-1, QUANTI-Blue™ solution, and lipopolysaccharide 0111: B4 (LPS) were purchased from InvivoGen (San Diego, California, USA). Phorbol 12-myristate 13-acetate (PMA) and streptozotocin (STZ) were acquired from Merck (Kenilworth, UK). Zoletil 100 was obtained from Virbac Laboratories (Carros, France), Stroless was obtained from China Chemical and Pharmaceutical Co. (Taipei, Taiwan), and Atropine from Astar Pharmaceutical Co. (Hsinchu, Taiwan). Isoflurane was purchased from Panion and BF Biotech, Inc. (Taipei, Taiwan). Anti-CD31 antibody from Arigo (Hsinchu, Taiwan); anti-CD63 antibody from Abclonal (Woburn, Massachusetts, USA); anti-syntenin antibody, and anti-VEGF antibody were from Abcam (Cambridge, UK). All media and reagents used were of analytical grade, and cell culture assays were performed at 37 °C with 5% CO_2.

Preparation and Characterization of RJEVs

RJ was obtained in a crude, unprocessed form from controlled organic beekeepers in Kaohsiung, Taiwan. RJ was diluted at a ratio of 1:20 with PBS prior to applying the TOOLSharp cell culture media exosome extraction kit (New Taipei City, Taiwan), which was used according to the manufacturer's instructions. The RJEVs were resuspended in sterilized and filtered PBS and stored at −80 °C. Samples were never refrozen after use in vitro or in vivo. Protein content was profiled using LTQ-Orbitrap mass spectrometry (Thermo Fisher Scientific, Waltham, Massachusetts, USA). The size distribution and concentration of RJEVs were analyzed using nanoparticle tracking analysis (NTA, Particle Metrix, Inning am Ammersee, Germany), and their double-membrane structure was confirmed by transmission electron microscopy (TEM, Hitachi, Tokyo, Japan). The RJEV markers CD63 and syntenin were analyzed using Western blotting, consistent with the previously reported characterization of RJEVs.[25] The protein concentration of RJEVs was analyzed using a Qubit 4 Fluorometer (Thermo Fisher Scientific, Waltham, Massachusetts, USA). RJEVs were labeled with ExoSparkler Exosome Membrane Labeling Kit-Green EX01 dye (Dojindo, Kumamoto, Japan) and added to recipient cells according to the manufacturer's protocol to study their cellular uptake. Recipient cells were cultured to 70% confluence, treated with labeled RJEVs, and incubated for 24 h. DAPI blue staining was used to label cell nuclei. Cellular uptake was observed using a Zeiss LSM 700 confocal laser scanning microscope (Oberkochen, Germany). Furthermore, the content of endotoxin in RJEVs was tested in a chromogenic lyophilized amebocyte lysate (LAL) assay, following the manufacturer's instructions (ToxinSensor™ Endotoxin Detection System, GenScript, Nanjing, China). The detection limit of this assay was 0.01 EU/mL, and to avoid potential interference of RJEVs sample with the LAL test, endotoxin concentrations were validated by a spiking procedure.

Cell Culture and Stimulation

CCD966SK human dermal fibroblasts (BCRC, Hsinchu, Taiwan) were cultured in MEM supplemented with 1.5 g/L sodium bicarbonate, 0.1 mM NEAA, 100 U/mL Pen-Strep, 1 mM sodium pyruvate, and 10% FBS. Cells were stimulated with 25.5 mM glucose to mimic a high-glucose (HG) environment.

RAW-Blue™ cells (InvivoGen, San Diego, California, USA) were derived from murine macrophages (RAW 264.7) and designed to monitor the responses of NF-κB and AP-1. Cells were cultured in DMEM supplemented with 2 mM L-glutamine, 10% heat-inactivated FBS, 100 μg/mL Normocin™, and 100 U/mL Pen-Strep. Zeocin (200 μg/mL) was added to every other passage to maintain the selection pressure for NF-kB and AP-1. The cells were stimulated with lipopolysaccharide (LPS, 1 μg/mL) to mimic an inflammatory environment.

THP-1 (BCRC, Hsinchu, Taiwan) is a human leukemia monocyte cell line widely used to study immunology. THP-1 cells were cultured in RPMI 1640 medium supplemented with 2 mM L-glutamine, 1.5 g/L sodium bicarbonate, 4.5 g/L glucose, 10 mM HEPES, 1.0 mM sodium pyruvate, 10% FBS, and 100 U/mL Pen-Strep. Cells were incubated with 100

ng/mL PMA for 24 h to activate the signal transduction enzyme protein kinase C and induce macrophage differentiation in monocytic cell lines. LPS (1 μg/mL) was used to mimic an inflamed environment.

Fibronectin (ScienCell Research Laboratories, Carlsbad, California, USA) was dissolved in sterile PBS and filtered through a 0.22 μm sterile filter before being added to cover the entire surface of the cell culture dish. HUVECs (ScienCell Research Laboratories, Carlsbad, California, USA) were cultured in endothelial culture media (ScienCell Research Laboratories, Carlsbad, California, USA). Cells were stimulated with 25.5 mM glucose to mimic an HG environment.

Cell Viability Assay

To determine the effect of RJEVs on cell lines, the cells were cultured in 96-well plates until 95% confluence and then treated with various doses (0, 10, 20, 50, 100, and 500 μg/mL) of RJEVs in the presence or absence of HG or LPS for 24 h before the CellTiter 96® AQueous One Solution Cell Proliferation Assay (Promega, Madison, Wisconsin, USA).

Scratch Assay

The migration of RJEVs-treated fibroblasts and HUVECs in HG-stimulated media was assessed using scratch assays performed in 12-well plates with culture inserts (IBIDI, Gräfelfing, Germany). When the cells reached approximately 95% confluence, the wells were washed twice with HBSS and supplemented with 10 and 20 μg/mL of RJEVs for an hour, followed by HG stimulation for 24 h. Images were captured at 0, 8, and 24 h and analyzed using ImageJ software (National Institutes of Health, Bethesda, Maryland, USA).

Senescence Assay

A senescence β-galactosidase Staining Kit (Cell Signaling Technology, Danvers, Massachusetts, USA) was used to evaluate the expression of SA-β-gal in fibroblasts. CCD-966SK cells were pre-treated with 20 μg/mL of RJEVs for an hour before HG stimulation for 24 h. Cells were then visualized under an optical microscope and analyzed using ImageJ software.

COL1α1 ELISA Assay

The quantification of COL1α1 was assessed by human collagen type I alpha 1 ELISA Kit (E-EL-H0869; Elabscience Bionovation Inc., Houston, Texas, USA). The assay was performed according to the manufacturer's instructions and detected at 450 nm using the Multiskan SkyHigh photometer (Thermo Fisher Scientific, Waltham, Massachusetts, USA).

NF-κB Expression Assay

The activation of NF-κB and AP-1 was detected using the QUANTI-Blue™ assay (InvivoGen, San Diego, California, USA). This procedure was performed according to the manufacturer's instructions. LPS (1 μg/mL), RJEVs (20 μg/mL), and negative control (endotoxin-free water) were added to the cells and incubated for 16 h. After incubation, 20 μL of the induced RAW-Blue™ supernatant was added to a new flat-bottom 96-well plate, followed by 180 μL QUANTI-Blue™ solution. The plates were incubated for 5 h, and NFκB-SEAP levels were determined using a spectrophotometer at 620 nm.

Cytokine Expression Analysis

The Luminex Discovery Assay (R&D Systems, Minneapolis, Minnesota, USA) is a multi-analyte kit that can simultaneously detect multiple biomarkers. IL-1β/IL-1F2, IL-6, IL-8/CXCL8, and TNF-α were chosen as the target analytes. The assay was performed according to the manufacturer's instructions. The microparticles were resuspended in 100 μL of wash buffer and incubated on a shaker for 2 min at 800 rpm before analysis using a Luminex 200 (Luminex Corporation, Austin, Texas, USA).

Tube Formation Assay

Tube formation is an essential assay for determining the capacity of HUVECs to form capillary-like structures in vitro. Briefly, the Matrigel® matrix (Corning, Corning, New York, USA) was plated at 50 μL/well in a pre-cooled 96-well plate on ice and

incubated for at least 30 min to promote gelation. HUVECs were seeded onto a Matrigel®-coated 96-well plate at a density of 2×10^5 cells/well and incubated with serum-free culture medium containing RJEVs for an hour before HG stimulation. Capillary-like structures were observed under an inverted light microscope (Nexcope, Ningbo, Zhejiang, China).

Porcine Wound Model and Wound Healing Assessment

Landmark pigs were obtained, and experiments were performed at Kaohsiung Veterans General Hospital. All animal care and surgical protocols were approved by the IACUC (2022–2023-A059) and followed the "Guideline for the Care and Use of Laboratory Animals" from the Council of Agriculture Executive Yuan. They were maintained in controlled environments and were offered normal pig feed before the induction of diabetes. The diabetes porcine model was induced using a combination of streptozotocin (STZ) injections and a continuous high-fat diet regimen. Specifically, two doses of STZ (40 mg/kg each) were administered, and the animals were simultaneously maintained on a high-fat diet consisting of 53% general feed, 10% salad oil, and 37% sucrose. The pigs underwent wound incision when they reached the diabetes standard (fasting blood sugar level > 100 mg/dL). General anesthesia was induced using Zoletil 100 (3–5 mg/kg) via intramuscular injection mixed with Stroless (2–8 mg/kg) and Atropine (0.02–0.05 mg/kg). Inhalational anesthesia was maintained throughout the surgical procedure using isoflurane (Panion & BF Biotech Inc., Taipei, Taiwan) and oxygen. Hair was removed using an electrical razor and sequentially sterilized with 75% ethanol and 7.5% povidone-iodine solution. A transparent film with 2×2 cm^2 holes was used to standardize the wound size. Skin incisions were made along the traced lines using a scalpel, followed by a putty knife to ensure consistent wound depth. After saline washing, RJEVs were applied to two wound beds, and the control wounds were left untreated. The wounds were then covered with Tegaderm dressings (3M, Saint Paul, Minnesota, USA) and additional protective bandages. The wounds were cleaned, and the dressings were changed every four days. Changes in body weight and food intake were monitored daily. Wound closure was monitored by photography. A ruler was placed around the wound to visually measure wound closure. Changes in the wound area were calculated as a percentage of the original wound area.[28] ImageJ software was used to measure the wound size.

Tissue Section Staining

Tissues from porcine wound sites were fixed in 4% formaldehyde buffered with PBS and embedded in paraffin wax. Embedded constructs were cut into very fine tissue sections, deparaffinized in xylene and a ladder of ethanol (50% - 100%), and hydrated before staining. The tissues were stained with Hematoxylin and Eosin (Abcam, Cambridge, UK) and visualized using an inverted optical microscope (U-RFL-T, Olympus, Tokyo, Japan).

Statistical Analysis

All data are presented as mean ± standard deviation (SD). All data were tested for normality using the Shapiro–Wilk test. GraphPad Prism version 9.5.0 for Windows (GraphPad Software, San Diego, California, USA) was used for analysis using Student's *t*-test. Statistical significance was considered at $*p < 0.05$, $**p < 0.01$, $***p < 0.001$.

Results

RJEVs Accelerate Migration and Decrease Cellular Senescence in High Glucose-Stimulated Human Dermal Fibroblasts

RJEVs were isolated and characterized using various techniques. LTQ-Orbitrap MS revealed the presence of MRJP1 in RJEVs. Nanoparticle tracking analysis (NTA) revealed their size distribution, with a peak at 118 ± 20 nm (Figure 1A), which lies within the expected range for extracellular vesicles as reported in the updated MISEV guidelines.[29] Transmission electron microscopy (TEM) confirmed in Figure 1B the double-membrane structure of RJEVs. Western blotting identified the presence of RJEVs markers, syntenin and CD63, further validating their characterization (Figure 1C). Endotoxin levels were below the accepted threshold for in vivo use, which was around 0.005 EU/mL (Supplementary Figure 2). Spiking the RJEVs samples with endotoxin achieved the acceptable spike recovery (78%).

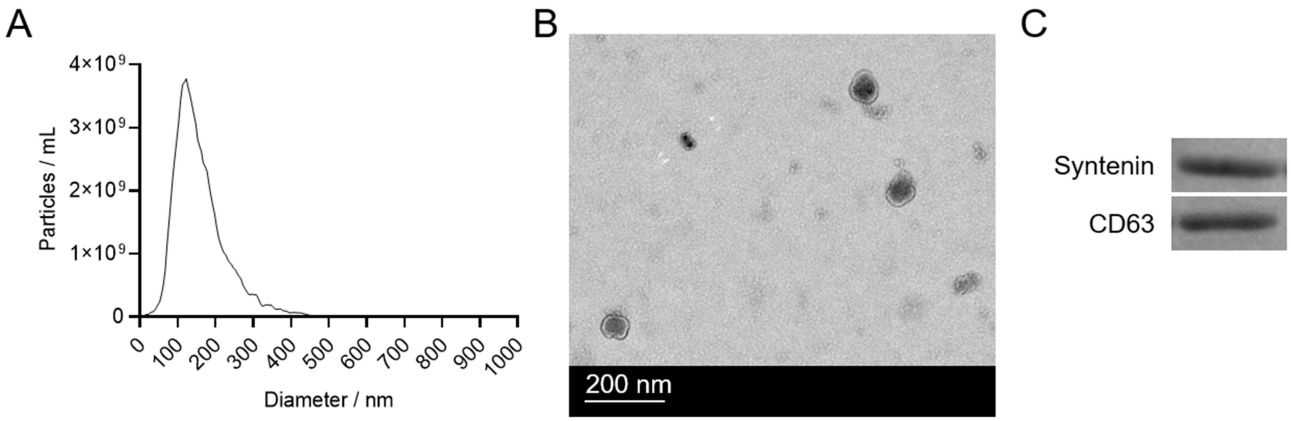

Figure 1 Characteristics of RJEVs. (**A**) NTA analysis of size and distribution. (**B**) TEM analysis of vesicle shape. (**C**) Western blot analysis of syntenin and CD63. n = 3.

The uptake of fluorescently labeled RJEVs by fibroblasts was observed, demonstrating their potential for cellular interaction (Figure 2A). The effects of RJEVs on fibroblasts under normal and high glucose (HG) conditions were investigated for 24 h. RJEVs were not cytotoxic to fibroblasts (Figure 2B). Moreover, HG stimulation decreased fibroblast viability by 34.4 ± 5.6% (Figure 2C), which was ultimately recovered by RJEVs treatment by 31.4 ± 4.4% at 10 μg and 30.7 ± 5.7% at 20 μg. In this study, RJEVs mitigated HG-induced cellular senescence by 24.7 ± 5.8% (Figure 2D and E). Fibroblasts create a new extracellular matrix (ECM) and collagen structure that assist other cells in wound healing. The results of the ELISA assay revealed that HG decreased human collagen type I alpha 1 (COL1α1) protein concentration by 28.6 ± 6.3%, while RJEVs increased COL1α1 protein concentration in HG-stimulated fibroblasts by 41.9 ± 7.6%, suggesting a potential role in maintaining ECM production and collagen synthesis (Figure 2F). Furthermore, RJEVs enhanced wound closure rates in fibroblasts by approximately 36.6 ± 4.6% compared to the HG group after 24 h (Figure 2G and H). Collectively, these findings indicate that RJEVs may have therapeutic potential for promoting wound healing and counteracting the detrimental effects of high glucose levels on fibroblasts.

RJEVs Decrease NF-κB Levels and Pseudopodia Formation in LPS-Stimulated Macrophages

The effects of RJEVs on macrophages (RAW-Blue™ cells) were examined, focusing on cellular uptake, viability, and anti-inflammatory properties. Fluorescent labeling techniques were employed to visualize the uptake of RJEVs by cells (Figure 3A). Dose-dependent RJEVs treatment showed no cytotoxicity towards macrophages, suggesting its suitability for cellular applications (Figure 3B). To simulate wound conditions in patients with diabetes, inflammation was induced in macrophages using LPS, a potent immune system activator. As shown in Figure 3C, treatment with 1 μg/mL LPS reduced cell viability by around 48.7 ± 4.3%, whereas treatment with 10 and 20 μg/mL RJEVs partially restored cell viability by approximately 21.7 ± 5.5% and 17.7 ± 4.4%, respectively. Moreover, 20 μg/mL RJEVs decreased NF-κB activity in LPS-stimulated cells by 21.3 ± 2.6% (Figure 3D), indicating an anti-inflammatory effect of the treatment. The increased cell body size observed in LPS-stimulated macrophages is a significant indicator of macrophage activation. This enlargement enhances phagocytic capacity and secretory function. Pseudopodia, which were also observed in LPS-stimulated macrophages, play crucial roles in cell motility, environmental exploration, and phagocytosis. Increased pseudopodia formation suggests heightened macrophage activity and readiness to respond to stimuli. In contrast, the reduced dendritic cell numbers and predominantly spherical or ovoid shapes observed upon RJEVs treatment indicated a less activated state, potentially leading to reduced inflammatory responses (Figure 3E). Collectively, these findings suggest that RJEVs can attenuate inflammation by reducing NF-κB-SEAP activity, potentially offering therapeutic benefits for wound healing in patients with diabetes.

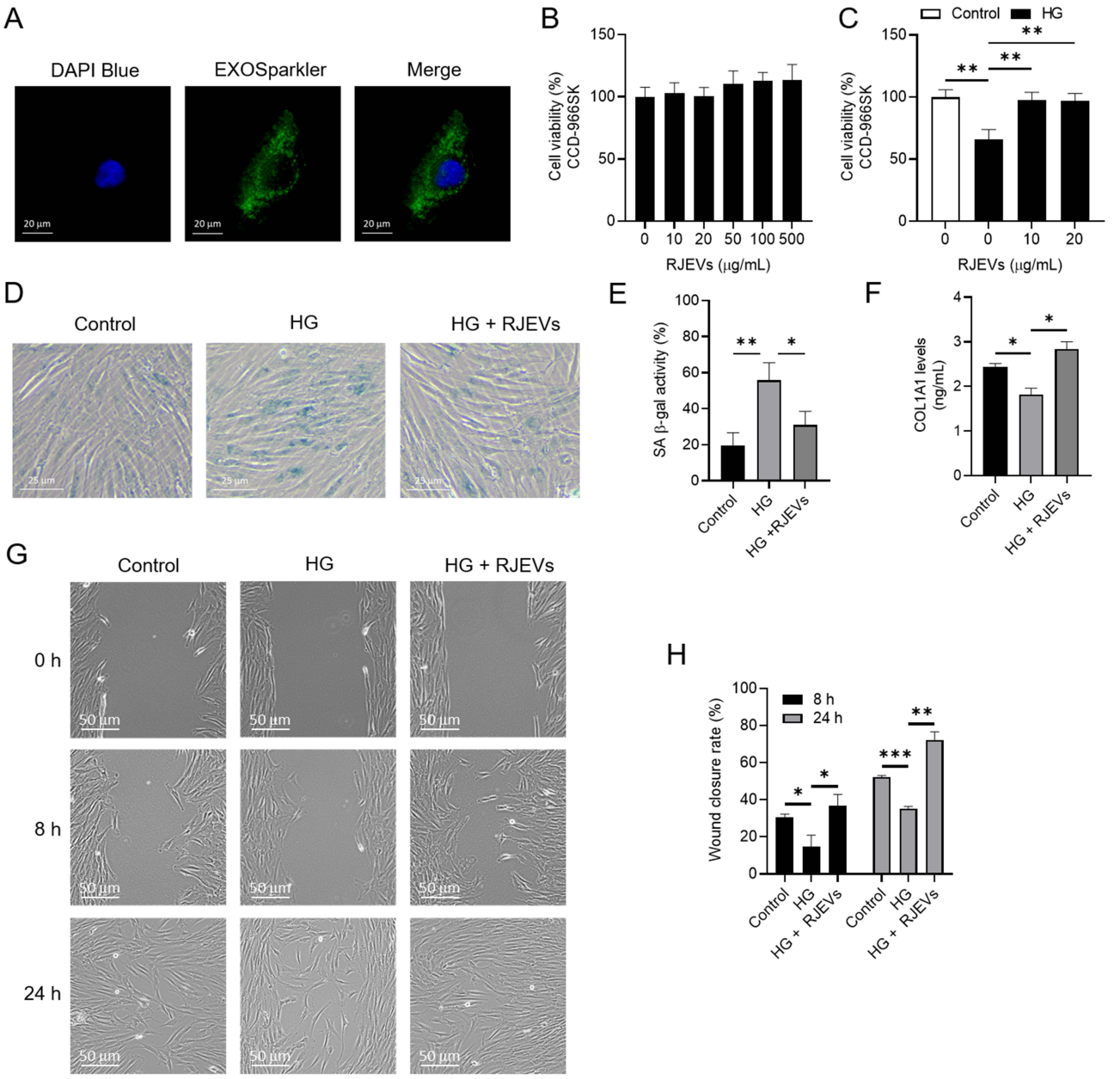

Figure 2 RJEVs accelerate migration rate while decreasing cellular senescence in high-glucose-stimulated fibroblasts. (**A**) Cellular uptake of RJEVs in fibroblasts was visualized by confocal microscopy. (**B**) MTS analysis of fibroblast cellular viability with 0, 10, 20, 50, 100, 500 μg/mL RJEVs treatments for 24 h. (**C**) MTS assay of fibroblasts cellular viability with 0, 10, 20 μg/mL RJEVs treatment in the presence or absence of HG stimulation for 24 h. (**D**) SA β-galactosidase assay of fibroblasts stimulated with HG and treated with 20 μg/mL RJEVs. (**E**) Quantitative analysis of SA-β-gal activity from three independent experiments. (**F**) COL1A1 expression in fibroblasts stimulated with HG and treated with 20 μg/mL RJEVs. (**G**) Migration rate of fibroblasts stimulated with HG and treated with 20 μg/mL RJEVs. (**H**) Quantitative analysis of wound closure rate expressed in three independent experiments. Data are shown as mean ± SD of three independent biological replicates. n = 3. *p < 0.05, **p < 0.01, ***p < 0.001; HG samples are compared to control and HG + RJEVs samples are compared to HG samples.

RJEVs Lower Inflammatory Cytokines in THP-1 Cells

This study further investigated the effects of RJEVs on THP-1 cells, a human monocytic cell line widely used in immune response research. THP-1 cells were treated with 100 ng/mL PMA to induce differentiation. Cellular uptake of RJEVs was verified using fluorescent labeling techniques, which demonstrated the internalization of RJEVs by THP-1 cells (Figure 4A). Notably, the introduction of RJEVs did not compromise the cell viability (Figure 4B), indicating their

https://doi.org/10.2147/IJN.S541042

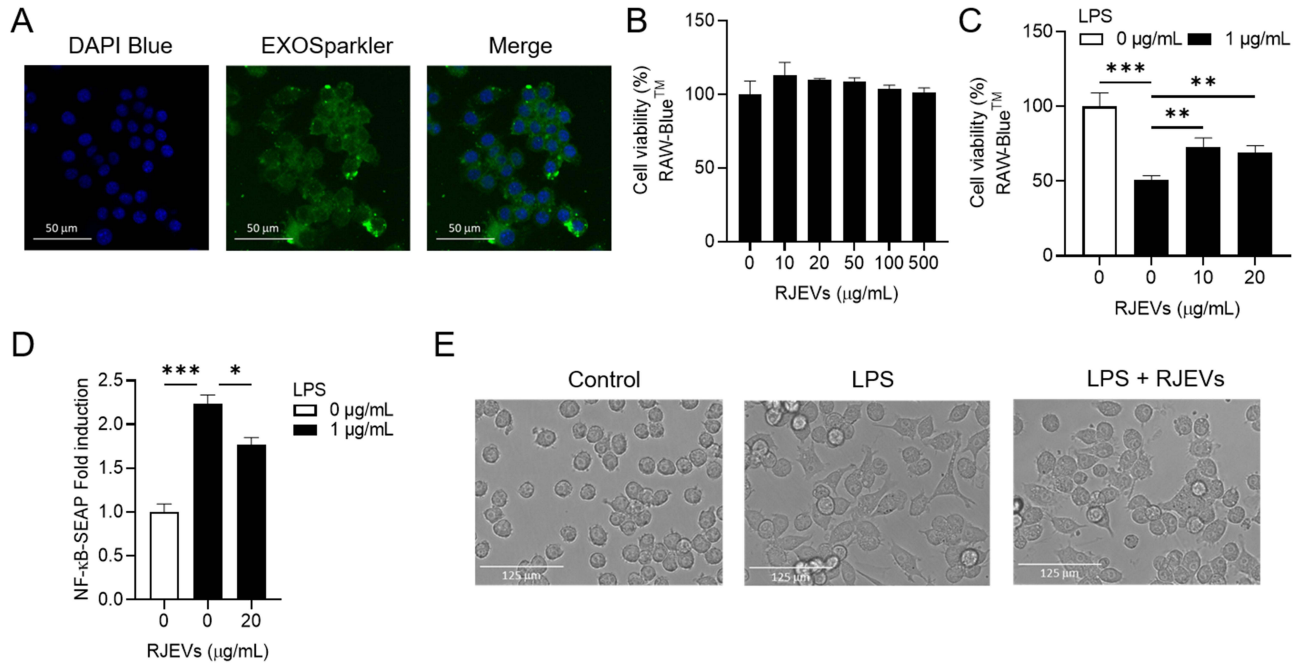

Figure 3 RJEVs decrease NF-κB activity and pseudopodia formation in LPS-stimulated macrophages. (**A**) Cellular uptake of RJEVs in RAW-Blue™ cells was visualized by confocal microscopy, (**B**) MTS analysis of RAW-Blue™ cellular viability with 0, 10, 20, 50, 100, 500 μg/mL RJEVs treatments for 24 h, (**C**) MTS assay of RAW-Blue™ cellular viability with 0, 10, 20 μg/mL RJEVs treatment with or without 1 μg/mL LPS stimulation for 24 h, (**D**) NF-κB activity analysis by QUANTI-Blue™, (**E**) Morphology of RAW-Blue™ cells stimulated with 1 μg/mL LPS and treated with 20 μg/mL RJEVs. Data are shown as mean ± SD of three independent biological replicates. n = 3. **p* < 0.05, ***p* < 0.01, ****p* < 0.001; LPS samples are compared to control and LPS + RJEVs samples are compared to LPS samples.

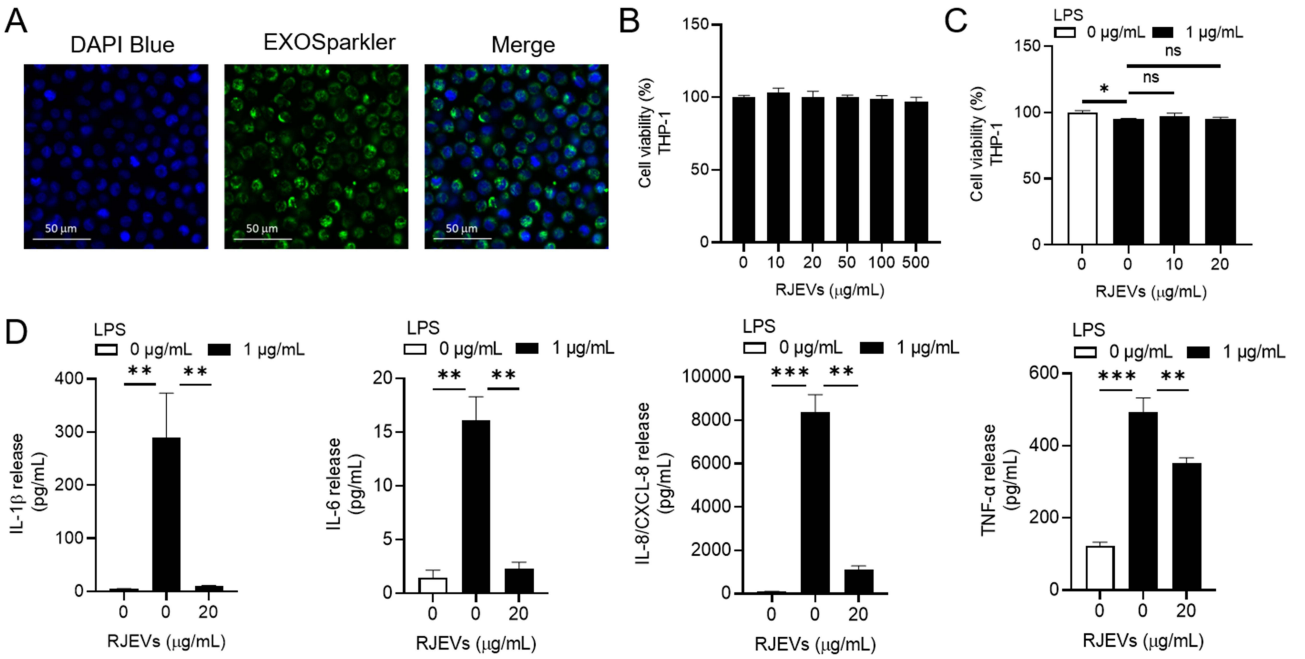

Figure 4 RJEVs reduce inflammatory cytokine expressions in THP-1 cells. (**A**) Cellular uptake of RJEVs in THP-1 cells was visualized by confocal microscopy, (**B**) MTS analysis of THP-1 cellular viability with 0, 10, 20, 50, 100, 500 μg/mL RJEVs treatments for 24 h, (**C**) MTS assay of THP-1 cellular viability with 0, 10, 20 μg/mL RJEVs treatment with or without 1 μg/mL LPS stimulation for 24 h, (**D**) Cytokine expression of IL-1β, IL-6, IL-8, and TNF-α in THP-1 cells stimulated with 1 μg/mL LPS and treated with 20 μg/mL RJEVs was analyzed using a multiplex cytokine assay kit. Data are shown as mean ± SD of three independent biological replicates. n = 3. ns = not significant, **p* < 0.05, ***p* < 0.01, ****p* < 0.001; LPS samples are compared to control and LPS + RJEVs samples are compared to LPS samples.

potential for therapeutic application. To simulate an inflammatory environment, THP-1 cells were exposed to 1 μg/mL LPS, and no significant changes in cell viability were observed in LPS-induced THP-1 cells in the presence or absence of RJEVs (Figure 4C). As depicted in Figure 4D, multiplex cytokine assay results demonstrated a significant increase in IL-1β, IL-6, IL-8, and TNF-α release after stimulation with 1 μg/mL LPS by 289.6 ± 73.6 pg/mL, 16.1 ± 2.4 pg/mL, 8359.6 ± 682.6 pg/mL, and 493.1 ± 43.2 pg/mL, respectively. Subsequent treatment with 20 μg/mL RJEVs resulted in a consequential decrease in the levels of each cytokine, with IL-1β by 96.5 ± 1.27%, IL-6 by 85.9 ± 0.65%, IL-8 by 86.7 ± 16.2%, and TNF-α by 27.4 ± 1.5%. This observation suggests that RJEVs possess potent anti-inflammatory properties and can modulate the immune response, even in the presence of strong pro-inflammatory stimuli. In conclusion, the data in Figure 4 demonstrate that RJEVs effectively mitigated inflammation in THP-1 cells, as evidenced by reduced pro-inflammatory cytokine production. The anti-inflammatory effects of RJEVs suggest their potential to facilitate wound healing in patients with diabetes, where chronic inflammation is a significant obstacle to tissue repair and regeneration.

RJEVs Increase Tube Formation in HUVECs

HUVECs were selected for angiogenesis studies because they closely mimic in vivo blood vessel behavior and offer a reliable and replicable system for vascular research. Figure 5A depicts the internalization of RJEVs by HUVECs, visualized using the EXOSparkler Exosomes Membrane Labeling Kit-Green for RJEVs and DAPI blue for cell nuclei. Neither RJEVs nor HG stimulation caused cytotoxicity in HUVECs (Figure 5B and C). Notably, Figure 5D and E reveal that HG stimulation reduced tube formation by approximately 52.9 ± 6.1%, whereas the introduction of RJEVs to HG-stimulated HUVECs restored tube formation by around 36.1 ± 2.4%. The number of branch points decreased by 24.8 ± 5.2% under HG stimulation, and RJEVs treatment increased it by 17.5 ± 7.5% (Supplementary Figure 3). Moreover, RJEVs accelerated HUVECs migration under HG conditions by around 35.7 ± 5.6% after 24 h compared to HG-stimulated HUVECs (Figure 5F and G). To investigate the molecular mechanisms underlying RJEV-induced angiogenesis, Western blotting was performed to assess the expression of two crucial angiogenic markers, VEGF and CD31. As shown in Figure 5H, HG stimulation diminished the expression of both VEGF and CD31, whereas the addition of 20 μg/mL RJEVs restored their expression. These observations indicate that RJEVs can enhance angiogenesis under hyperglycemic conditions, which is crucial for wound healing in diabetic patients with compromised angiogenesis. The ability of RJEVs to mitigate the adverse effects of HG levels on endothelial cell function and angiogenesis underscores their potential therapeutic applications in addressing diabetic complications associated with impaired vascular function.

RJEVs Accelerate Wound Healing in STZ-Induced Diabetic Porcine

The wound-healing efficacy of RJEVs was assessed using a streptozotocin (STZ)-induced diabetic porcine model. Wound closure was documented using digital images captured on days 0, 10, 21, 31, and 42 (Figure 6A). The RJEVs treatment groups showed significantly improved wound closure rates compared to the control group, with 27 ± 8.3% and 30.8 ± 7% closure rates observed on days 21 and 31, respectively (Figure 6B). By day 42, the difference in wound closure between the control and RJEVs treatment groups increased to 32.5 ± 7.2%, highlighting the potential of RJEVs to accelerate wound healing under diabetic conditions. Histological evaluation was performed on day 42 (Figure 6C), and the results highlighted key differences in tissue regeneration. The control group exhibited incomplete epidermal coverage and poorly organized collagen deposition. RJEVs-treated wounds displayed complete re-epithelialization and a fully developed dermal matrix, consistent with advanced healing. Qualification data of epidermal thickness showed an increase of 37.2 ± 12.5% (Supplementary Figure 4).

These findings provide substantial evidence of the potential of RJEVs to accelerate wound healing in diabetic conditions. The synergistic effect of RJEVs offers a promising approach to enhance wound healing in patients with diabetes, addressing a significant clinical challenge in wound management.

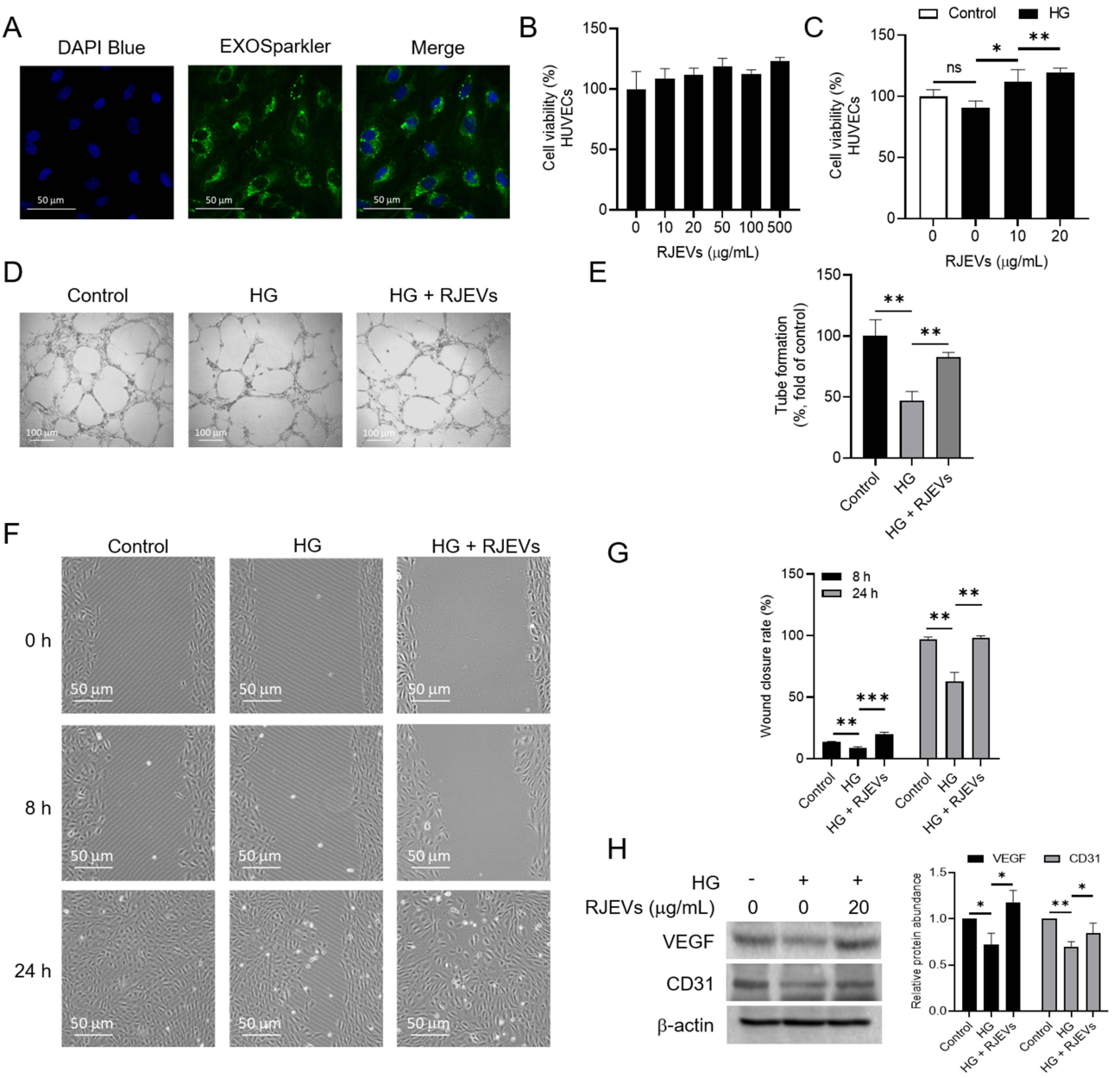

Figure 5 RJEVs increase tube formation in HUVECs. (**A**) Cellular uptake of RJEVs in HUVECs was visualized by confocal microscopy, (**B**) MTS assay of HUVECs cellular viability with 0, 10, 20, 50, 100, 500 μg/mL RJEVs treatment, (**C**) MTS assay of HUVECs cellular viability with 0, 10, 20 μg/mL RJEVs treatment in the presence or absence of HG stimulation for 24 h, (**D**) HUVECs tube formation with 20 μg/mL RJEVs in the presence of absence of HG stimulation, (**E**) Quantitative analysis of tube formation of three independent experiments, (**F**) Migration rate of HUVECs stimulated with HG and treated with 20 μg/mL RJEVs, (**G**) Quantitative analysis of wound closure rate expressed of three independent experiments, (**H**) Western blot of VEGF and CD31 in HUVECs stimulated with HG and treated with 20 μg/mL RJEVs. Data are shown as mean ± SD of three independent biological replicates. n = 3. ns = not significant, *$p < 0.05$, **$p < 0.01$, ***$p < 0.001$; HG samples are compared to control and HG + RJEVs samples are compared to HG samples.

Discussion

This study demonstrates that RJEVs significantly enhance diabetic wound healing. They promote fibroblast migration and collagen expression, stimulate angiogenesis via VEGF upregulation, and reduce inflammation through suppression of NF-κB activity and pro-inflammatory cytokines. These findings suggest that RJEVs may serve as a promising biotherapeutic approach for chronic wound management in patients with diabetes. Rather than establishing definitive clinical efficacy, our results provide preclinical evidence of potential utility and warrant further investigation using advanced wound models. Our research substantially expands the potential of EV-based wound therapy by integrating

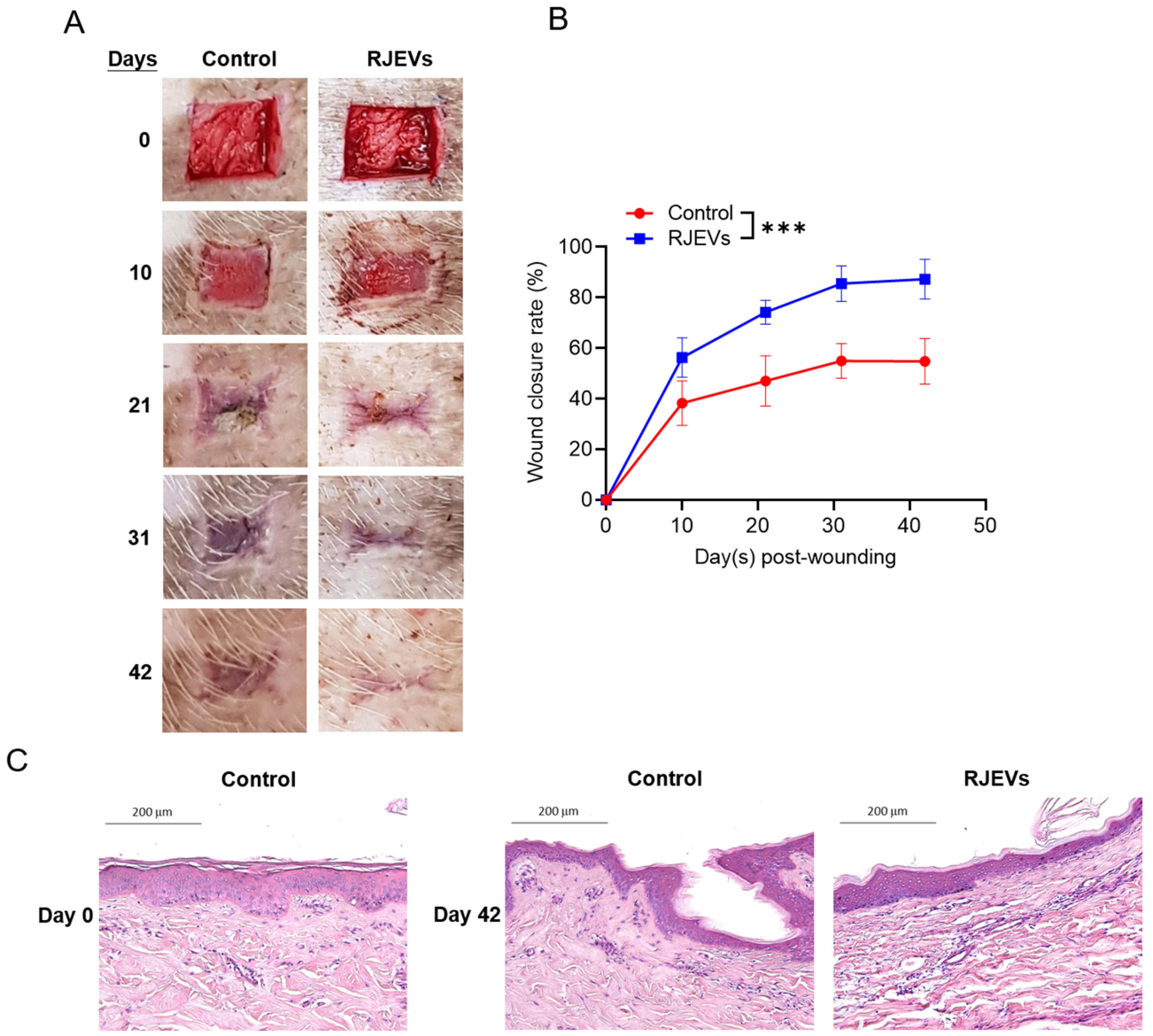

Figure 6 Accelerated wound healing in diabetic porcine after RJEVs treatment. (**A**) The rate of wound healing from day 0 (wound induction day) to day 42 in 4 porcines. (**B**) Quantitative measurement of each wound is represented by at least 4 wounds. (**C**) Histopathological examination of H&E-stained wound tissue (day 0) and healed tissue (day 42). Data are shown as mean ± SD of four independent biological replicates. n = 4. ***$p < 0.001$; all samples are compared to control.

recent advancements in stem cell–derived EVs. Mesenchymal stem cell (MSC)–derived EVs have been shown to facilitate re-epithelialization, enhance angiogenesis, and modulate immune responses via miRNAs and protein delivery.[30–39] These effects mirror the multifunctional benefits observed with RJEVs and further support the feasibility of EV-mediated regeneration.

Compared with conventional therapies, RJEVs may offer a complementary alternative by harnessing bioactive molecules to support tissue repair and recovery. Their natural origin and scalability make them attractive candidates for wound-healing applications, although their therapeutic consistency and safety require additional validation. Beyond diabetic wounds, RJEVs could potentially be explored in other chronic wound settings, including burn injuries, pressure ulcers, and surgical incisions; however, such extensions remain speculative until supported by additional mechanistic and translational studies.

Previous studies have explored the incorporation of RJEVs into hydrogel systems as delivery vehicles and supportive environments for tissue regeneration to enhance their therapeutic potential for wound healing. Ramírez et al investigated

https://doi.org/10.2147/IJN.S541042

integrating RJEVs into collagen hydrogels to enhance retention at wound sites and prolong therapeutic effects.[26] Tan et al combined RJEVs with a photocrosslinked SerMA hydrogel to achieve gradual release and accelerate wound healing by modulating inflammation and vascular impairment.[40] These studies underscore the potential of hydrogel-RJEVs composites for chronic wound healing applications. Future research could investigate different hydrogels to fine-tune RJEV release for specific wound types. This may lead to more effective and personalized wound therapy. In addition, other EV delivery formats are under active development, including microneedle patches and sprayable formulations. Dissolving or hydrogel-forming microneedles have been shown to deliver vesicles with ROS-scavenging, antibacterial, and repair-promoting properties in diabetic models.[41–43] Meanwhile, sprayable hydrogel dressings allow for even coverage of irregular wound beds and may enhance patient compliance.[44,45] These strategies highlight the versatility of RJEVs and suggest that their future integration into engineered biomaterials could increase their translational potential.

Another critical aspect to consider is the potential mechanism underlying RJEVs-mediated wound healing. Although our study suggests that RJEVs modulate fibroblast migration, collagen formation, and endothelial function, it remains unclear whether their effects are mediated by direct signaling or through the cargo delivery of bioactive molecules such as miRNAs and proteins. Saadeldin et al identified 29 mature and 17 novel miRNAs in RJEVs. Among these, miR-31 and miR-200b are particularly relevant to the wound healing process.[27] In particular, miR-31 and miR-200b were expressed at lower levels in diabetic wounds than in nondiabetic wounds.[46,47] Huang et al developed an engineered miR-31 exosome that promoted angiogenesis, fibrogenesis, and reepithelialization.[47] Another study by Wang et al observed a decrease in miR-200b in db/db mice.[48] After injecting an miR-200b mimic into wounds, accelerated healing was observed through a decrease in inflammation and an increase in pro-angiogenic effects. In the literature, the presence of MRJP1 in RJEVs has been characterized as the most abundant MRJP. MRJP1 is known for its antioxidant properties, which help reduce oxidative stress and prevent DNA damage, thereby enhancing cell viability.[49] Furthermore, Álvarez et al reported an increase in multipotency in mammalian stem cells by MRJP1.[50] The anti-aging properties of MRJP1 have also been highlighted, as they promote growth factor signaling pathways that extend the lifespan of model organisms. Subsequent research should explore the specific mechanisms of RJEVs wound healing in diabetic models.

Although RJEVs show potential, several challenges remain before they can be clinically applied. The batch-to-batch variability of royal jelly, which is affected by floral source, season, and processing, must be standardized and controlled.[51,52] Safety concerns, including the potential immunogenicity of cross-kingdom vesicles, also require rigorous preclinical assessment. Future research on delivery systems, molecular mechanisms, and safety is essential to determine whether RJEVs can progress from experimental use to translational wound therapy.

Conclusions

In conclusion, this study highlights the potential of RJEVs as a novel and promising approach for enhancing diabetic wound healing. By simultaneously modulating fibroblast migration, inflammatory resolution, and angiogenesis, RJEVs offer a multifaceted therapeutic strategy that addresses the key pathological features of diabetic wounds. While these findings highlight their therapeutic potential, further studies are needed to delineate the underlying mechanisms, verify safety, and evaluate clinical feasibility before translating them into innovative, nature-derived wound management strategies in the future.

Abbreviations

RJ, Apis mellifera royal jelly; EVs, extracellular vesicles; RJEVs, Apis mellifera royal jelly-derived extracellular vesicles; MRJPs, major royal jelly proteins; NTA, nanoparticle tracking analysis; TEM, transmission electron microscopy; HG, high glucose; ECM, extracellular matrix; LPS, lipopolysaccharide.

Ethics Approval and Informed Consent

All animal care and surgical protocols were approved by the IACUC (2022-2023-A059) and performed at Kaohsiung Veterans General Hospital.

Consent for Publication

All authors have consented to data publication.

Acknowledgments

We would like to thank the Center for Research and Resources and Development of Kaohsiung Medical University for assistance with Confocal Imaging and Nanoparticle Tracking Analysis.

Funding

This research was supported by the National Science and Technology Council, Taiwan (grant number NSTC 113-2320-B-037-015-MY3) and the NSYSU-KMU Joint Research Project (grant number NSYSU-KMU-114-P31).

Disclosure

The authors declare no conflicts of interest or personal relationships that could influence this work.

References

1. Diao W, Li P, Jiang X, Zhou J, Yang S. Progress in copper-based materials for wound healing. *Wound Repair Regen*. 2023;32:314–322. doi:10.1111/wrr.13122
2. Verdolino DV, Thomason HA, Fotticchia A, Cartmell S. Wound dressings: curbing inflammation in chronic wound healing. *Emerg Top Life Sci*. 2021;5(4):523–537. doi:10.1042/ETLS20200346
3. Holl J, Kowalewski C, Zimek Z, et al. Chronic diabetic wounds and their treatment with skin substitutes. *Cells*. 2021;10(3):655. doi:10.3390/cells10030655
4. Tang Y, Zhang MJ, Hellmann J, Kosuri M, Bhatnagar A, Spite M. Proresolution therapy for the treatment of delayed healing of diabetic wounds. *Diabetes*. 2013;62(2):618–627. doi:10.2337/db12-0684
5. Burgess JL, Wyant WA, Abdo Abujamra B, Kirsner RS, Jozic I. Diabetic wound-healing science. *Medicina*. 2021;57(10):1072. doi:10.3390/medicina57101072
6. Park JH, Kim S, Hong HS, Son Y. Substance P promotes diabetic wound healing by modulating inflammation and restoring cellular activity of mesenchymal stem cells. *Wound Repair Regen*. 2016;24(2):337–348. doi:10.1111/wrr.12413
7. Kita A, Saito Y, Miura N, et al. Altered regulation of mesenchymal cell senescence in adipose tissue promotes pathological changes associated with diabetic wound healing. *Commun Biol*. 2022;5(1):310. doi:10.1038/s42003-022-03266-3
8. Feng J, Wang J, Wang Y, et al. Oxidative stress and lipid peroxidation: prospective associations between ferroptosis and delayed wound healing in diabetic ulcers. *Front Cell Dev Biol*. 2022;10:898657. doi:10.3389/fcell.2022.898657
9. Shimoyama Y, Nakamura N, Kawaguchi T, Okumura K. Complications after surgery in hemodialysis patients: a comparison between diabetic and non-diabetic patients. *Dial Transplant*. 2009;38(10):412–414. doi:10.1002/dat.20356
10. Liang Y, He J, Guo B. Functional hydrogels as wound dressing to enhance wound healing. *ACS Nano*. 2021;15(8):12687–12722. doi:10.1021/acsnano.1c04206
11. Mirhaj M, Labbaf S, Tavakoli M, Seifalian AM. Emerging treatment strategies in wound care. *Int Wound J*. 2022;19(7):1934–1954. doi:10.1111/iwj.13786
12. Fujii A, Kobayashi S, Kuboyama N, et al. Augmentation of wound healing by royal jelly (RJ) in streptozotocin-diabetic rats. *Jpn J Pharmacol*. 1990;53(3):331–337. doi:10.1254/jjp.53.331
13. Rashidi MK, Mirazi N, Hosseini A. Effect of topical mixture of honey, royal jelly and olive oil-propolis extract on skin wound healing in diabetic rats. *Wound Med*. 2016;12:6–9. doi:10.1016/j.wndm.2015.12.001
14. Lin Y, Zhang M, Lin T, et al. Royal jelly from different floral sources possesses distinct wound-healing mechanisms and ingredient profiles. *Food Funct*. 2021;12(23):12059–12076. doi:10.1039/D1FO00586C
15. Huang X, Xiu L, An Y, et al. Preventive effect of royal jelly and 10-HDA on skin damage in diabetic mice through regulating keratinocyte Wnt/β-catenin and pyroptosis pathway. *Mol Nutr Food Res*. 2024;68(19):2400098. doi:10.1002/mnfr.202400098
16. Oršolić N, Jazvinšćak Jembrek M. Royal jelly: biological action and health benefits. *Int J Mol Sci*. 2024;25(11):6023. doi:10.3390/ijms25116023
17. Kumar R, Thakur A, Kumar S, Hajam YA. Royal jelly a promising therapeutic intervention and functional food supplement: a systematic review. *Heliyon*. 2024;10:e37138. doi:10.1016/j.heliyon.2024.e37138
18. Li S, Tao L, Yu X, Zheng H, Wu J, Hu F. Royal jelly proteins and their derived peptides: preparation, properties, and biological activities. *J Agric Food Chem*. 2021;69(48):14415–14427. doi:10.1021/acs.jafc.1c05942
19. Queen Elizabeth Hospital. A study to determine whether nanocrystalline silver dressing, manuka honey dressing and conventional dressing are effective in the treatment of diabetic foot ulcer. NLM identifier: NCT02577900. Last update posted April 16, 2019. Available from: https://clinicaltrials.gov/study/NCT02577900. Accessed October 13, 2025.
20. Siavash M, Shokri S, Haghighi S, Mohammadi M, Shahtalebi MA, Farajzadehgan Z. The efficacy of topical royal jelly on diabetic foot ulcers healing: a case series. *J Res Med Sci*. 2011;16(7):904. PMID: 22279458.
21. Siavash M, Shokri S, Haghighi S, Shahtalebi MA, Farajzadehgan Z. The efficacy of topical royal jelly on healing of diabetic foot ulcers: a double-blind placebo-controlled clinical trial. *Int Wound J*. 2015;12:137–142. doi:10.1111/iwj.12063
22. Khazaei M, Ansarian A, Ghanbari E. New findings on biological actions and clinical applications of royal jelly: a review. *J Diet Suppl*. 2018;15(5):757–775. doi:10.1080/19390211.2017.1363843

23. Malkin EZ, Bratman SV. Bioactive DNA from extracellular vesicles and particles. *Cell Death Dis*. 2020;11(7):584. doi:10.1038/s41419-020-02803-4
24. Correa R, Caballero Z, De León LF, Spadafora C. Extracellular vesicles could carry an evolutionary footprint in interkingdom communication. *Front Cell Infect Microbiol*. 2020;10:76. doi:10.3389/fcimb.2020.00076
25. Álvarez S, Contreras-Kallens P, Aguayo S, et al. Royal jelly extracellular vesicles promote wound healing by modulating underlying cellular responses. *Mol Ther Nucleic Acids*. 2023;31:541–552. doi:10.1016/j.omtn.2023.02.008
26. Ramírez OJ, Alvarez S, Contreras-Kallens P, Barrera NP, Aguayo S, Schuh CM. Type I collagen hydrogels as a delivery matrix for royal jelly derived extracellular vesicles. *Drug Deliv*. 2020;27(1):1308–1318. doi:10.1080/10717544.2020.1818880
27. Saadeldin IM, Tanga BM, Bang S, et al. MicroRNA profiling of royal jelly extracellular vesicles and their potential role in cell viability and reversing cell apoptosis. *Funct Integr Genomics*. 2023;23(3):200. doi:10.1007/s10142-023-01126-9
28. Kuo TY, Huang CC, Shieh SJ, et al. Skin wound healing assessment via an optimized wound array model in miniature pigs. *Sci Rep*. 2022;12(1):445. doi:10.1038/s41598-021-03855-y
29. Welsh JA, Goberdhan DC, O'Driscoll L, et al. Minimal information for studies of extracellular vesicles (MISEV2023): from basic to advanced approaches. *J Extracell Vesicles*. 2024;13(2):e12404. doi:10.1002/jev2.12404
30. Zhang W, Ling Y, Sun Y, Xiao F, Wang L. Extracellular vesicles derived from mesenchymal stem cells promote wound healing and skin regeneration by modulating multiple cellular changes: a brief review. *Genes*. 2023;14(8):1516. doi:10.3390/genes14081516
31. Marofi F, Alexandrovna KI, Margiana R, et al. MSCs and their exosomes: a rapidly evolving approach in the context of cutaneous wounds therapy. *Stem Cell Res Ther*. 2021;12(1):597. doi:10.1186/s13287-021-02662-6
32. Casado-Díaz A, Quesada-Gómez JM, Dorado G. Extracellular vesicles derived from mesenchymal stem cells (MSC) in regenerative medicine: applications in skin wound healing. *Front Bioeng Biotechnol*. 2020;8:146. doi:10.3389/fbioe.2020.00146
33. Narauskaitė D, Vydmantaitė G, Rusteikaitė J, et al. Extracellular vesicles in skin wound healing. *Pharmaceuticals*. 2021;14(8):811. doi:10.3390/ph14080811
34. Saadh MJ, Ramirez-Coronel AA, Saini RS, et al. Advances in mesenchymal stem/stromal cell-based therapy and their extracellular vesicles for skin wound healing. *Human Cell*. 2023;36(4):1253–1264. doi:10.1007/s13577-023-00904-8
35. Yang B, Lin Y, Huang Y, Zhu N, Shen Y-Q. Extracellular vesicles modulate key signalling pathways in refractory wound healing. *Burns Trauma*. 2023;11:tkad039. doi:10.1093/burnst/tkad039
36. Wang Y, Ding H, Bai R, et al. Exosomes from adipose-derived stem cells accelerate wound healing by increasing the release of IL-33 from macrophages. *Stem Cell Res Ther*. 2025;16(1):80. doi:10.1186/s13287-025-04203-x
37. Feng H, Gong S, Liu J, et al. Adipose-derived stem cell exosomes: mechanisms and therapeutic potentials in wound healing. *Biomarker Res*. 2025;13:88. doi:10.1186/s40364-025-00801-2
38. Jia Q, Zhao H, Wang Y, Cen Y, Zhang Z. Mechanisms and applications of adipose-derived stem cell-extracellular vesicles in the inflammation of wound healing. *Front Immunol*. 2023;14:1214757. doi:10.3389/fimmu.2023.1214757
39. An Y, Lin S, Tan X, et al. Exosomes from adipose-derived stem cells and application to skin wound healing. *Cell Proliferation*. 2021;54(3):e12993. doi:10.1111/cpr.12993
40. Tan D, Zhu W, Liu L, et al. In situ formed scaffold with royal jelly-derived extracellular vesicles for wound healing. *Theranostics*. 2023;13:2811. doi:10.7150/thno.84665
41. Wu D, Wu X, Luan Q, et al. Dynamic hydrogel-integrated microneedle patch with extracellular vesicles encapsulation for wound healing. *Chem Eng J*. 2024;493:152252. doi:10.1016/j.cej.2024.152252
42. Qi F, Xu Y, Zheng B, et al. The core-shell microneedle with probiotic extracellular vesicles for infected wound healing and microbial homeostasis restoration. *Small*. 2024;20(46):2401551. doi:10.1002/smll.202401551
43. Wang X, Cheng W, Su J. Research progress of extracellular vesicles-loaded microneedle technology. *Pharmaceutics*. 2024;16(3):326. doi:10.3390/pharmaceutics16030326
44. Vipin C, Kumar GV. Exosome laden sprayable thermo-sensitive polysaccharide-based hydrogel for enhanced burn wound healing. *Int J Biol Macromol*. 2025;290:138712. doi:10.1016/j.ijbiomac.2024.138712
45. Liu B, Chen L, Huang C, et al. A sprayable exosome-loaded hydrogel with controlled release and multifunctional synergistic effects for diabetic wound healing. *Mater Today Bio*. 2025;34:102159. doi:10.1016/j.mtbio.2025.102159
46. Mulholland EJ, Dunne N, McCarthy HO. MicroRNA as therapeutic targets for chronic wound healing. *Mol Ther Nucleic Acids*. 2017;8:46–55. doi:10.1016/j.omtn.2017.06.003
47. Dangwal S, Stratmann B, Bang C, et al. Impairment of wound healing in patients with type 2 diabetes mellitus influences circulating microRNA patterns via inflammatory cytokines. *Arterioscler Thromb Vasc Biol*. 2015;35:1480–1488. doi:10.1161/ATVBAHA.114.305048
48. Huang J, Yu M, Yin W, et al. Development of a novel RNAi therapy: engineered miR-31 exosomes promoted the healing of diabetic wounds. *Bioact Mater*. 2021;6:2841–2853. doi:10.1016/j.bioactmat.2021.02.007
49. Wang HJ, Sin CH, Yang SH, Hsueh HM, Lo WY. miR-200b-3p accelerates diabetic wound healing through anti-inflammatory and pro-angiogenic effects. *Biochem Biophys Res Commun*. 2024;731:150388. doi:10.1016/j.bbrc.2024.150388
50. Mureşan CI, Dezmirean DS, Marc BD, Suharoschi R, Pop OL, Buttstedt A. Biological properties and activities of major royal jelly proteins and their derived peptides. *J Funct Foods*. 2022;98:105286. doi:10.1016/j.jff.2022.105286
51. Khalfan Saeed Alwali Alkindi F, El–Keblawy A, Lamghari Ridouane F, Bano Mirza S. Factors influencing the quality of Royal jelly and its components: a review. *Cogent Food Agric*. 2024;10(1):2348253. doi:10.1080/23311932.2024.2348253
52. Ma C, Ma B, Li J, Fang Y. Changes in chemical composition and antioxidant activity of royal jelly produced at different floral periods during migratory beekeeping. *Food Res Int*. 2022;155:111091. doi:10.1016/j.foodres.2022.111091